A New Supernova Remnant Candidate and an Associated Outflow in the Sagittarius C Region

Takeshi Go Tsuru,[1] Masayoshi Nobukawa,[1] Hiroshi Nakajima,[2] Hironori Matsumoto,[1] Katsuji Koyama,[1] Shigeo Yamauchi,[3]

[1]*Department of Physics, Graduate School of Science, Kyoto University, Sakyo-ku, Kyoto, 606-8502*
tsuru@cr.scphys.kyoto-u.ac.jp

[2]*Department of Earth and Space Science, Graduate School of Science, Osaka University, Toyonaka, Osaka, 560-0043*

[3]*Faculty of Humanities and Social Sciences, Iwate University, 3-18-34 Ueda, Morioka, Iwate 020-8550*

(Received 2008 August 5; accepted 2008 September 15)

Abstract

We present the Suzaku results on a new candidate of a supernova remnant (SNR) in the Sagittarius C region. We detected diffuse X-rays of an elliptical shape (G 359.41−0.12) and chimney-like structure (the Chimney), both of which are fitted with a thin thermal model of $k_{\rm B}T \sim 1$ keV temperature. The absorption columns are same between these two structures, indicating the both are located at the same distance in the same line of sight. The narrow band image and one-dimensional profile of S XV Kα at 2.45 keV show that the Chimney is emanating from G 359.41−0.12. Therefore these two sources are physically connected with each other. The sum of thermal energies of the Chimney and G 359.41−0.12 is estimated to be 1.4×10^{50} ergs, typical for a Galactic SNR. G 359.41−0.12 is likely a new SNR candidate and the Chimney is an associated outflow.

Key words: Galaxy: center — ISM: supernova remnants — ISM: bubbles — X-rays: ISM

1. Introduction

The Galactic center diffuse X-rays (GCDX) is characterized by many K-shell lines from highly ionized atoms covering a large area of the Galactic center (GC) (Koyama et al. 1989; Yamauchi et al. 1990; Koyama et al. 1996; Koyama et al. 2007c). This indicates the presence of a large scale plasma of temperature $k_{\rm B}T$= 1–10 keV. If this plasma is truly diffuse and extending in the GC, it contains a huge thermal energy ($\sim 10^{53-54}$ ergs). Since the high temperature

plasma can not be confined by the Galactic gravity, it may escape from the GC in a short time ($\sim 10^5$ yr), the escape time scale. Thus, we need a huge energy input of $\sim 10^{48-49}$ ergs yr^{-1}.

One plausible hypothesis is a multiple (~ 1000) supernovae in the GC region. However, only a few supernova remnants (SNRs) had so far been detected in the X-ray band. This situation has been changing after the launch of the Suzaku satellite. The X-ray Imaging Spectrometer (XIS) combined with the X-Ray Telescope (XRT) onboard Suzaku has superior performance, a large collecting area, a stable and low non-X-ray background (NXB) and a high energy-resolution. In order to make the most of these superiority, a significant amount of the Suzaku observation time are allocated to the GC. As a result, Suzaku has discovered several new SNRs located in the Sagittarius (Sgr) A, Sgr B1, B2 and Sgr D regions (Koyama et al. 2007b; Nobukawa et al. 2008; Sawada et al. 2009; Mori et al. 2008a; Mori et al. 2008b).

Sgr C is one of the brightest radio complexes in the GC. There are well-defined non-thermal radio filaments (NTFs), some compact and evolved H II regions, far-IR and submillimeter sources, and giant molecular clouds (Liszt 1985; Tsuboi et al. 1991; Lis & Caristrom 1994; Liszt & Spiker 1995). Accordingly, a rich variety of X-ray features may be expected. However, the X-ray studies have been concentrated on the diffuse 6.4 keV line emission (Fe I Kα) (Murakami et al. 2001; Yusef-Zadeh et al. 2007; Nakajima et al. 2009); few results on thermal diffuse emissions have been reported so far. Thus, we conducted the studies of thermal emissions from the Sgr C region with Suzaku. Nakajima et al. (2009) reported the 6.4 keV clumps in the Sgr C region. Using the same data set, we searched for thermal features, and found clumpy emissions of thin thermal nature. We report on the results and discuss the origin of the diffuse thermal X-rays.

Following Nakajima et al. (2009), "the east" and "the north" are referred as the positive Galactic longitude side, and the positive Galactic latitude side, respectively. The distance to Sgr C is assumed to be 8.5 kpc. The solar abundance and photoelectric absorption cross-section are taken from the tables of Anders & Grevesse (1989) and Balucinska-Church & McCammon (1992), respectively.

2. X-Ray Data Processing

The Sgr C region was observed with the XIS from 2006 Feb. 20 to 23, and the XIS data were obtained with the 3×3 and 5×5 modes and with the normal clocking mode. The pointing position was R.A.=$17^{\rm h}44^{\rm m}37\overset{\rm s}{.}30$, Decl.= $-29^\circ28'10\overset{''}{.}2$ (J2000.0). The XIS consists one (XIS 1) back-illuminated (BI) CCD and three sensors (XIS 0, 2 and 3) front-illuminated (FI) CCDs. The detailed descriptions of the Suzaku satellite, XRT, and XIS can be found in Mitsuda et al. (2007), Serlemitsos et al. (2007) and Koyama et al. (2007a), respectively.

The data reduction and screenings are essentially the same as Nakajima et al. (2009),

but we applied the calibration database (CALDB) released on 2008 July 2[1]. For the data processing, we selected X-ray events by subtracting the NXB from the raw data. Since the flux of the NXB depends on the geomagnetic cut-off rigidity (COR) (Tawa et al. 2008), we applied the COR-sorted NXB (using the data sets provided by the XIS team[2]), to become the same COR distribution as that in the Sgr C observation. We exclude the data of the corners in the field of view (FOV) illuminated by the onboard calibration sources of ^{55}Fe.

3. Analysis and Results

3.1. Imaging of Thermal Emissions

We searched for a thin thermal plasma in the images of S XV Kα lines at 2.45 keV (for a plasma temperature of $k_{\rm B}T \lesssim 1$ keV) and/or Fe XXV Kα lines at 6.68 keV (for a plasma temperature of $k_{\rm B}T \gtrsim 1$ keV). For the data processing and analysis of the imaging study, we co-added the four CCD (XIS 0, 1, 2, and 3) data and made the exposure and vignetting corrections. In the Fe XXV Kα image (6.6–6.8 keV), we found no significant structure. However, in the narrow band image of the S XV Kα line at 2.45 keV (2.40–2.50 keV), we found a bright extended source at $(l, b) = (359.^{\circ}41, -0.^{\circ}12)$, hence designated as G 359.41−0.12 hereafter (figure 1). Another diffuse emission has a chimney-like structure extending from G 359.41−0.12 to the north direction, which we call as "the Chimney". Two known bright point sources, 1E 1740.7−2942 ($\sim 5 \times 10^{-10}$ergs cm^{-2} s^{-1}) and A1742-294 ($\sim$ 3–6 $\times 10^{-10}$ergs cm^{-2} s^{-1}), are located outside the FOV in the western and south-east directions, respectively (e.g., Sidoli et al. 1999). The contamination due to the stray-light from the two sources is only $\sim 2-3\%$ of the flux of the Chimney in the energy band of 2.40–2.50 keV (Serlemitsos et al. 2007). Thus, the Chimney is a real structure.

To see if the Chimney is connected with G 359.41−0.12 quantitatively, we constructed an one-dimensional surface brightness profile at 2.45 keV with the length of 18.′5 along the green rectangle in figure 1. The origin of the profile is defined at the northern side of the box. The background level was obtained from the background regions of the spectra of the Chimney and G 359.41−0.12 shown in figure 1. The 2.45 keV profile shown in figure 2 clarifies that the surface brightness from G 359.41−0.12 to the Chimney are well above the background level. On the other hand, the profile is not smooth but has two dips at distances of $\sim 3.'5$ and $\sim 7'$.

As mentioned above, a bright source 1E 1740.7−2942 is located outside the FOV in the western direction. A possible radio SNR having a size of 22 pc×10 pc, G 359.07−0.02, is cataloged in LaRosa et al. (2000). Thus, the western excess would be due to the XRT PSF (point spread function) tail of 1E 1740.7−2942 and/or eastern edge of G 359.07−0.02. At the time of writing this paper, Suzaku already made a pointing observation of the western adjacent

[1] http://www.astro.isas.jaxa.jp/suzaku/caldb/

[2] http://www.astro.isas.jaxa.jp/suzaku/analysis/xis/nte/

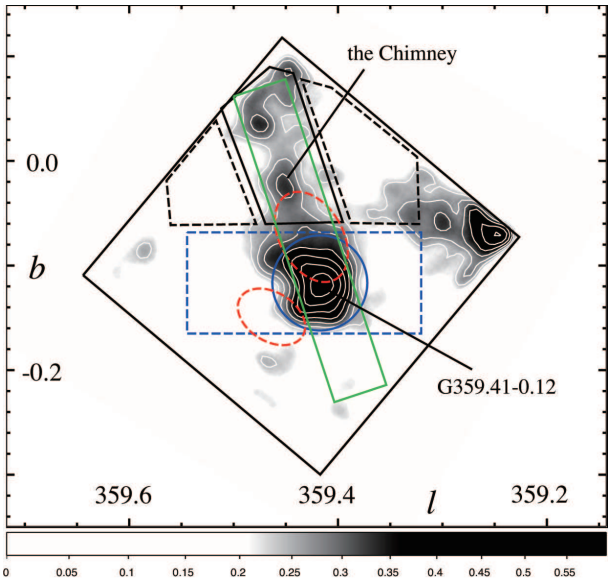

Fig. 1. The 2.45 keV-line (S XV Kα) image in the energy band of 2.40–2.50 keV after the smoothing with the Gaussian kernel of 60 pixels (1.′04). Contour levels are set at (4.2, 4.9, 5.7, 6.6, 7.8, 9.0, 10.6, 12.3, 14.4, 16.8) $\times 10^{-7}$ ph s^{-1} cm^{-2} arcmin^{-2}. The typical 1σ error is 0.5×10^{-7} ph s^{-1} cm^{-2} arcmin^{-2}. We collected the source and background spectra of the Chimney from the regions shown with solid blue and dashed black lines, respectively. Extraction of the source spectra of G 359.41−0.12 were made from the region given with the solid line, while its background spectra were obtained from the region of dashed blue lines but the source area (solid bule circle) was excluded. Also the data within the red dashed ellipses (M 359.43−0.07 and M 359.47−0.15) were excluded to minimize the contamination from the strong 6.4 keV emission line and its associated continuum. The green box with the size of $18.'5 \times 3'$ gives the region for the one-dimensional profile shown in figure 2.

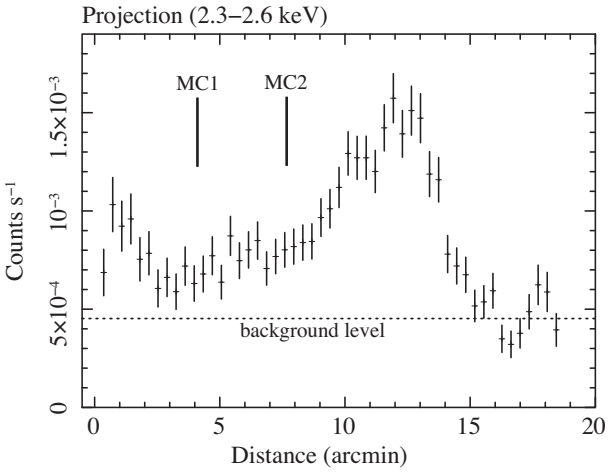

Fig. 2. One-dimensional surface brightness profile at 2.45 keV (2.30–2.60 keV) along the green box connecting the Chimney with G 359−0.12 (figure 1). The origin of the profile is defined at the northern side of the rectangle. The dotted line shows the background level obtained from the the background regions for the Chimney and G 359.41−0.12 indicated in figure 1. "MC 1" and "MC 2" show the positions of ridges of the molecular clouds crossing the Chimney (see figure 4).

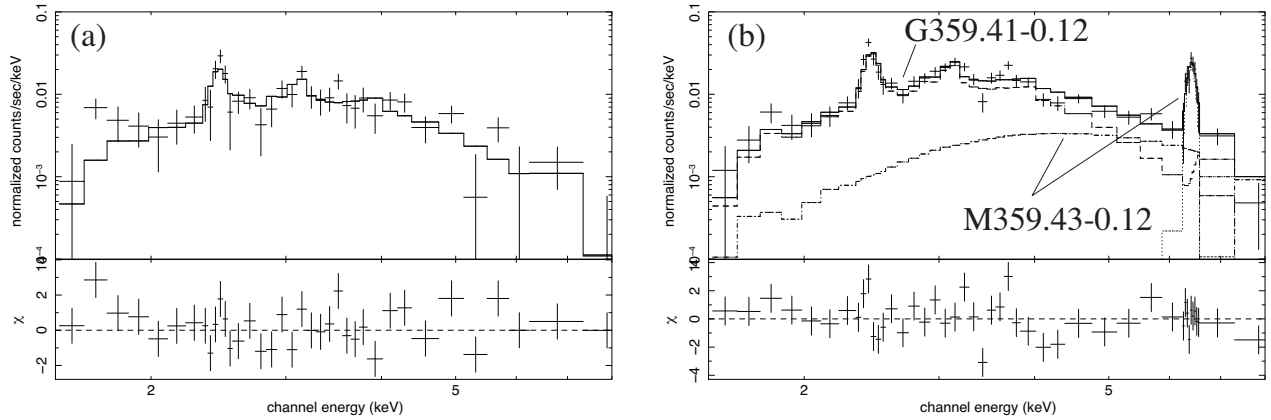

Fig. 3. The background subtracted FIs spectra of (a) the Chimney and (b) G 359.41−0.12 with the best fit model spectra. Although, we simultaneously fitted the FIs and BI spectra, only the FI results are given for brevity.

region. However, the exposure time was only ~ 20 ksec, and hence it is not clear whether the excess near the western edge of the FOV is a real excess or a spill over of these X-ray sources. We therefore will not discuss on this excess in this paper.

3.2. Spectral Analyses

In the spectral studies, we treated the co-added FIs (XIS 0,2,3) data and BI (XIS 1) data separately because the response function of FIs and BI are significantly different. The spectra were extracted from the regions shown in figure 1. Since the surface brightness of the GCDX, the most significant background component, depends on the Galactic latitude, the background regions for the Chimney and G 359.41−0.12 were selected to have the same latitude as those of corresponding source areas. The energy-dependent vignetting were corrected by multiplying the effective-area ratio of the source region to the corresponding background area for each energy bin. Since the 6.4 keV clumps, M 359.43−0.07 and M 359.47−0.15 have a strong 6.4 keV-line and associated continuum emission (Nakajima et al. 2009), we excluded the regions of these 6.4 keV clumps from both of the source and background areas, in order to minimize the contamination of the clumps.

The background (the GCDX) subtracted FIs spectrum of the Chimney is shown in figure 3 (a). We see two conspicuous emission lines from highly ionized atoms, S XV Kα (2.45 keV) and Ar XVII Kα (3.12 keV). We, therefore, fitted the spectrum by a thin thermal plasma model in collisional ionization equilibrium affected by photoelectric absorption (`vapec` and `wabs` models in XSPEC, respectively). The fit was reasonably good as is shown in table 1.

The background (the GCDX) subtracted spectra of G 359.41−0.12 shows prominent 6.4 keV emission lines from Fe I Kα as well as S XV Kα and Ar XVII Kα. This 6.4 keV line emission come from a 6.4 keV clump, M 359.43−0.12, which is located inside the source region of G 359.41−0.12 and hence difficult to specially exclude (Nakajima et al. 2009).

Table 1. Best-fit parameters of the Chimney and G 359.41−0.12

Parameters	the Chimney	G 359.41−0.12
$N_{\rm H}$ (10^{22} cm^{-2})	10.1 (8.6–12.2)	12.0 (11.5–12.4)
$k_{\rm B}T$ (keV)	1.15 (0.93–1.37)	0.90 (0.84–0.94)
$Z_{\rm S}$, Z_{Ar} ($Z_\odot$) †	1.73 (1.11–2.65)	1.72 (1.51–2.07)
$f_{\rm X}$♯ (thermal) (ergs cm^{-2} s^{-1})	3.23×10^{-13}	3.11×10^{-13}
$f_{\rm X}$♯ (power-law) (ergs cm^{-2} s^{-1})	···	2.39×10^{-13}
χ^2/d.o.f.	74.9/55	128.4/91

Notes. – The values in parentheses represent the 90% confidence intervals.
†The values of $Z_{\rm S}$ and $Z_{\rm Ar}$ are fixed to one another. Z of the other elements are fixed to the solar values. ♯Observed (absorption not corrected) flux at the 1.5–8.0 keV band.

The bight 6.4 keV clumps of M 359.43−0.07 and M 359.47−0.15, locating near G 359.41−0.12 and M 359.43−0.12, have essentially the same spectrum (Nakajima et al. 2009). Thus, assuming M 359.43−0.12 also has the same spectrum, we added a model of the fixed absorption column, photon index and equivalent widths of the best-fit of M 359.43−0.07 and M 359.47−0.15, and fit with the same model as the Chimney (a thin thermal model). The fit was acceptable as is shown in table 1. We further examined how the results of G 359.41−0.12 depend on the spectral shape of the M 359.43−0.12, by changing the model parameters within the errors. Then we found no significant change of the results; only the errors of the best-fit parameters of G 359.41−0.12 become larger by a factor of ~ 1.5.

4. Discussion

We discovered two diffuse X-ray sources with the 2.45 keV emission line (S XV Kα), G 359.41−0.12 and the Chimney. There is a well-defined non-thermal radio filament, G 359.45−0.06, running north-western direction in the Sgr C region (Liszt 1985; Liszt & Spiker 1995). However, the position angle of G 359.45−0.06 disagree with that of the Chimney by $\sim 40^\circ$, and hence the Chimney is not related to G 359.45−0.06 (figure 4). In the followings, we discuss the structure and origin of the plasmas.

4.1. Plasma Parameters

We first derived physical parameters of the Chimney and G 359.41−0.12, summarized in table 2. We assumed the Chimney and G 359.41−0.12 have the plasmas of an cylinder with the diameter of 7.4 pc (3.′0) and length of 20 pc (8.′0), and an ellipsoid with the dimensions of 8.6 pc× 8.6 pc × 12.4 pc ($3.'5 \times 3.'5 \times 5.'0$), respectively.

The plasma temperatures give sound velocities of $C_{\rm s} = 560$ km s^{-1} and 480 km s^{-1} for the Chimney and G 359.41−0.12, respectively. Hence, dividing the length or major axis by the sound velocities, we can estimate the dynamical time scales of the Chimney and G 359.41−0.12

Table 2. Physical parameters of the Chimney and G 359.41−0.12. *

Parameters	the Chimney	G 359.41−0.12
$\int n_e n_{\rm H} dV$ (cm^{-3})	4.9×10^{57}	1.3×10^{58}
V (pc^3)	8.5×10^2	4.8×10^2
$n_{\rm e}$ (cm^{-3})	$0.49 f^{-1/2}$	$1.1 f^{-1/2}$
M ($M_\odot$)	$14 f^{1/2}$	$14 f^{1/2}$
$E_{\rm th}$ (ergs)	$7.6 \times 10^{49} f^{1/2}$	$5.9 \times 10^{49} f^{1/2}$
$L_{\rm X}$♮ (ergs s^{-1})	2.2×10^{34}	3.9×10^{34}

Notes. – The distance is assumed to be 8.5 kpc. M, $E_{\rm th}$ and f are the mass, thermal energy and filling factor of the plasma, respectively. The other notations refer to table 1.
♮Unabsorbed luminosity between 1.5-8.0 keV.

to be 4.0×10^4 yr and 2.5×10^4 yr.

4.2. Physical Connection of the Chimney and G 359.41−0.12

We discuss if the plasmas of the Chimney and G 359.41−0.12 are connected with each other. The one-dimensional profile in figure 2 suggests that the X-ray emission continuously distributes between the two objects without break. The absorption columns of the Chimney and G 359.41−0.12 are almost identical at $N_{\rm H}$=(10-12)$\times 10^{22}$ cm^{-2}, suggesting that these two sources are at the same distance in the same line of sight. The temperatures and metal abundances of these sources are essentially the same. Therefore, we can infer that the Chimney and G 359.41−0.12 are physically connected with a similar nature.

4.3. Absorption by Molecular Clouds

Figure 4 shows ^{13}CO emission over the range −84 to −24 km s^{-1} overlaid on the X-ray image at 2.45 keV (Liszt & Spiker 1995). Anti-correlation among the four molecular clouds (MC 1, 2, 3, 4) and X-ray emission is clearly seen. The positions of MC 1 and MC 2 agree well with the two dips seen in the one-dimensional profile (figure 2). The hydrogen column densities of MC 1 and MC 2 estimated from the ^{13}CO emission are $N_{\rm H} \sim 2 \times 10^{22}$ cm^{-2} ($\sim$ 40% absorption at 2.45 keV). The unabsorbed counting rates plus the background level are obtained to be $\sim 8 \times 10^{-4}$ and $\sim 1.0 \times 10^{-3}$ counts s^{-1} at the position of MC 1 and MC 2, respectively. Thus, we can assume that MC 1 and MC 2 are located in front of the Chimney and absorb the X-ray emission; the dips would be due to the absorption by the molecular clouds and the unabsobed one-dimensional profile in the Chimney would decrease monotonically from G 359.41−0.12 without a significant dip. This result enforces the idea that G 359.41−0.12 and the Chimney are physically connected with each other (section 4.2).

Figure 4 also shows that the surface brightness at the 2.45 keV band is low at the positions of MC 3 and MC 4. The column densities of MC 3 and MC 4 obtained from the ^{13}CO

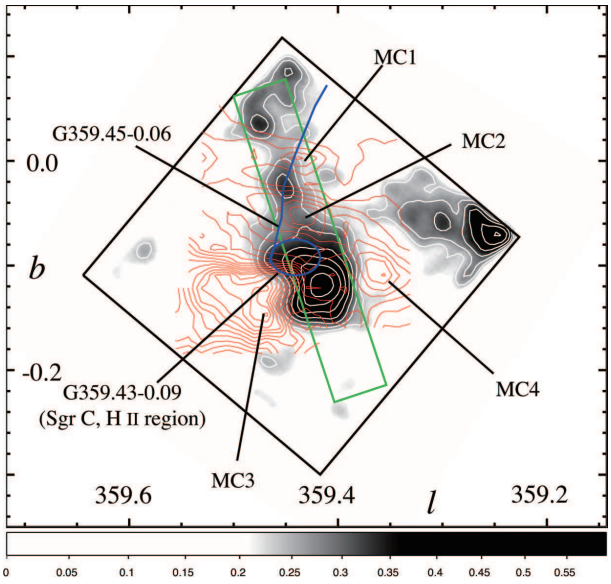

Fig. 4. The contours of ^{13}CO at -84 to -24 km s^{-1} (red) and the schematic diagram of the radio continuum sources of G 359.45−0.06 and G 359.43−0.09 (blue) are overlaid on the 2.45 keV-line (S XV Kα) image. The radio data are adopted from Liszt & Spiker (1995). MC 1, 2, 3, and 4 indicate the molecular clouds. The region for the one-dimensional profile in figure 2 is shown with the green box ($18\farcm5 \times 3'$).

emission are $N_{\rm H}\sim 7\times10^{22}$ cm^{-2} and $\sim 3\times10^{22}$ cm^{-2}, respectively. Thus, one can explain the anti-correlation would be due to the absorption by MC 3 ($\sim 80\%$) and MC 4 ($\sim 50\%$), as applied to MC 1 and MC 2. On the other hand, since the shapes of MC 3 and MC 4 trace the rim of G 359.41−0.12 well, the other possibility is that the molecular clouds block the plasma to expand further out. Since the surface brightness in the region of MC 3 and MC 4 is very low, further deep observation is necessary to clarify these two possibilities.

4.4. Origin of the Plasmas

First, we discuss the origin as star clusters. The observed X-ray luminosities of G 359.41−0.12 and the Chimney are (2–4)$\times10^{34}$ ergs s^{-1} in the 1.5–8 keV band. These luminosities are comparable with or higher than those of the Arches ($\sim 3\times10^{34}$ ergs s^{-1}) and Quituplet ($\sim 4\times10^{33}$ ergs s^{-1}) clusters, the X-ray brightest star clusters in the Galaxy (Tsujimoto et al. 2007; Wang et al. 2006). The canonical metal abundance of the Galactic H II regions obtained with X-ray spectroscopies is 0.3 solar (e.g., Getman et al. 2005), while G 359.41−0.12 and the Chimney have metal abundances of $1\sim2$ solar. There is a radio bright H II region, G 359.43−0.09 (Sgr C) as shown in figure 4 (Liszt & Spiker 1995). However, the peak position of G 359.41−0.12 is $2\farcm4$ shifted from that of G 359.43−0.09. Thus, it is unlikely that the X-rays of G 359.41−0.12 and the Chimney come from the H II regions.

A pulsar wind nebula and jet from a compact source are also unlikely as the origin of the Chimney and G 359.41−0.12, because a power law model failed to fit the observed spectra.

The X-ray luminosity, temperature, and the other physical parameters of G 359.41−0.12 and the Chimney are consistent with those of the SNRs detected in the GC (Nobukawa et al. 2008; Mori et al. 2008a; Sawada et al. 2009; Mori et al. 2008b). The sum of thermal energies of the Chimney and G 359.41−0.12 is 1.4×10^{50} ergs, typical for a Galactic SNR. Including the possible energy of the plasma bulk motion with the sound velocity into the total energy, it is still consistent with a single supernova. Therefore, we propose G 359.41−0.12 is a new SNR candidate and the Chimney is an outflow plasma from the SNR. The molecular clouds of MC 3 and MC 4 can block the plasma from expanding except in the northern direction. Then, the outflow in the direction of the north may be formed. In any case, the morphology of single SNR plus a chimney-like thermal outflow with the dimension of ~ 8 pc $\times$ 8 pc $\times$ 34 pc is very unusual as a SNR. Thus, further deep observation is highly required.

We are grateful to all members of the Suzaku hardware and software teams and the science working group. This work was supported by the Grant-in-Aid for the Global COE Program "The Next Generation of Physics, Spun from Universality and Emergence" from the Ministry of Education, Culture, Sports, Science and Technology (MEXT) of Japan. This work was also supported by Grants-in-Aid of Ministry of Education, Culture, Sports, Science and Technology No. 18204015 and 20340043. MN and HN are financially supported by the Japan Society for the Promotion of Science.

References

Anders, E., & Grevesse, N. 1989, Geochim. Cosmochim. Acta, 53, 197
Balucinska-Church, M., & McCammon, D. 1992, ApJ, 400, 699
Getman, K. V. 2005, ApJS, 160, 880
Koyama, K., Awaki, H., Kunieda, H., Takano, S., Tawara, Y. Yamauchi, S., Hatsukade, I., & Nagase, F. 1989, Nature, 339, 603
Koyama, K., Maeda, Y., Sonobe, T., Takeshima, T., Tanaka, Y., & Yamauchi, S. 1996, PASJ, 48, 249
Koyama, K., et al. 2007a, PASJ, 59, S23
Koyama, K., et al. 2007b, PASJ, 59, S221
Koyama, K., et al. 2007c, PASJ, 59, S245
LaRosa, T.N., Kassim, N.E., Lazio, T.J.W., & Hyman, S.D., 2000, AJ, 119, 207
Lis, D. C., & Caristrom, J. E. 1994, ApJ, 424, 189
Liszt, H. S. 1985, ApJL, 293, L65
Liszt, H. S., & Spiker, R. W. 1995, ApJS, 98, 259
Mitsuda. K. et al. 2007, PASJ, 59, S1
Mori. H., Tsuru, T. G., Hyodo, Y., Koyama, K. & Senda, A. 2008a, PASJ, 60, S183
Mori. H., Hyodo, Y., Tsuru, T. G., Nobukawa, M., & Koyama, K. 2008b, PASJ, submitted.
Murakami. H., Koyama, K., Tsujimoto, M., Maeda, Y., & Sakano, M. 2001, ApJ, 550, 297

Nakajima, H., Tsuru, T.G., Nobukawa, M., Matsumoto, H., & Koyama, K., Murakami, H., Senda, A., & Yamauchi, S. 2009, PASJ, in printing

Nobukawa, M., et al. 2008, PASJ, 60, S191

Sawada, M., Tsujimoto, M., Koyama, K., Law, C. J., Tsuru, T. G., Yamauchi, S., & Hyodo, Y. 2009, PASJ, in printing.

Serlemitsos, P. J. et al. 2007, PASJ, 59, 9

Sidoli, L., Mereghetti, S., Israel, G. L., Chiappetti, L., Treves, A., & Orlandini, M. 1999, ApJ, 525, 215

Tawa, N., Hayashida, K., Nagai, M., Nakamoto, H., Tsunemi, H., Yamaguchi, H., Ishisaki, Y., Miller, E. D., Mizuno, T., Dotani, T., Osaki, M, & Katayama, H. 2008, PASJ, 60, S11

Tsuboi, M., Kobayashi, H., Ishiguro, M., & Murata, Y. 1991, PASJ, 43, 27

Tsujimoto, M., Hyodo, Y., & Koyama, K. 2007, PASJ, 59, S229

Wang, Q. D., Dong, H., & Lang, C. 2006, MNRAS, 371, 38

Yamauchi, S., Kawada, M., Koyama, K., Kunieda, H., Tawara, Y., & Hatsukade, I. ApJ, 365, 532

Yusef-Zadeh, F., Muno, M., Wardle, M., & Lis, D. C. 2007, ApJ, 656, 847